

#### Available online at website: https://journal.bcrec.id/index.php/bcrec

### Bulletin of Chemical Reaction Engineering & Catalysis, 20 (3) 2025, 428-440



Original Research Article

# Salt-Assisted Mesostructured Cellular Foam (MCF) Silica Synthesis from Bagasse Bottom Ash for Enzymatic Starch Hydrolysis

#### Joni Agustian\*, Lilis Hermida

Department of Chemical Engineering, Universitas Lampung, Jl. S. Brodjonegoro No. 1, Gedong Meneng, Rajabasa, Bandar Lampung 35145, Province of Lampung, Indonesia.

Received: 16th April 2025; Revised: 26th May 2025; Accepted: 27th May 2025 Available online: 29th May 2025; Published regularly: October 2025



#### **Abstract**

Synthesis of MCF silica is presently conducted solely using TEOS and TMB, with the purpose of immobilizing amylolytic enzymes. Utilizing BBA and KCl to create the salt-assisted MCF silica present a viable option for converting a natural waste into an effective enzyme carrier, given its substantial silica content. The objectives were to produce the MCF silica, to employee the MCF silica as the glucoamylase carrier, and to know characteristics of the immobilized enzyme by conducting hydrolysis of starches. The carrier had surface area of 45.5 m<sup>2</sup>.g<sup>-1</sup>, pore volume of 0.12 cm<sup>3</sup>.g<sup>-1</sup>, pore size of 9.3 nm, and mesoporous silica type IV. Reduction in the carrier pore diameter and the medium to strong FTIR vibrations indicated free glucoamylase immobilization on carrier. The immobilization reached 88.5% efficiency, influenced by factors such as initial enzyme concentration, PO<sub>4</sub> buffer pH, and temperature, with agitation speed having a minor impact. This optimum value was obtained at the initial enzyme concentration of 9.0 mg.mL<sup>-1</sup>, agitation speed of 120 rpm, buffer pH of 5.5, and temperature of 30 °C. Hydrolysis of starches (tapioca, wheat, potato, corn) resulted in Dextrose Equivalent (DE) values ranging from 5.1% to 63.9%, with the immobilized glucoamylase showing better performance in potato starch hydrolysis (DE of 63.9%) and corn starch (DE of 45.6%). The use of BBA in synthesis of the salt-assisted MCF silica proved to be a viable and sustainable alternative for enzyme immobilization, with potential applications in industrial starch hydrolysis.

Copyright © 2025 by Authors, Published by BCREC Publishing Group. This is an open access article under the CC BY-SA License (https://creativecommons.org/licenses/by-sa/4.0).

**Keywords**: bagasse bottom ash; salt-assisted synthesis; dextrose equivalent; amylolytic enzyme; enzyme transporter efficiency

How to Cite: Agustian, J., Hermida, L. (2025). Salt-Assisted Mesostructured Cellular Foam (MCF) Silica Synthesis from Bagasse Bottom Ash for Enzymatic Starch Hydrolysis. Bulletin of Chemical Reaction Engineering & Catalysis, 20 (3), 428-440. (doi: 10.9767/bcrec.20379)

Permalink/DOI: https://doi.org/10.9767/bcrec.20379

#### 1. Introduction

Immobilizations of amylolytic enzymes have been made on natural and synthetic nanoparticles, however, their limited surface areas result in suboptimal immobilization efficiency. In contrast, mesoporous silicas having extensive surface areas provide a more effective way of attaching amylases compared to nanoparticles. Numerous mesoporous silica carriers either native, polymeric, or functionalized synthetic type, have immobilized glucoamylase,  $\alpha$ -amylase, and pullulanase enzyme.

Mesoporous cellular foam (MCF) silica synthesized from tetraethyl orthosilicate (TEOS) using 1,3,5-trimethylbenzene (TMB) as the swelling agent demonstrated high adsorption capacity for free SQzyme AGP glucoamylase [1-3] to yield the dextrose equivalent values of 1.74-76.30% (w/w). Adsorption of Aspergillus niger glucoamylase onto mesoporous silicas (MPS) prepared from TEOS and n-decane (the swelling agent) resulted in the immobilization efficiency of

Email: joni.agustian@eng.unila.ac.id (J. Agustian)

<sup>\*</sup> Corresponding Author.

79.05%, but the maximum reaction rate was slower than free glucoamylase during soluble starch hydrolysis [4]. Entrapment of Aspergillus glucoamylase within mono-polymeric mesoporous silica matrix made from TEOS and phenyltriethoxysilane in alcoholic environment, successfully conducted where immobilized enzyme exhibited an optimum unit activity comparable to that of free glucoamylase in saccharification of soluble starch [5].Functionalized MPS (synthesized from TEOS and n-decane) significantly enhanced performance of Aspergillus niger glucoamylase immobilization of free enzyme in phosphate buffer supplemented with phthalate resulted in recovery of 90-95% of free enzyme's activity [4,6]. Functionalized MCF silica (synthesized from TEOS and TMB modified with organosilanes) facilitated Aspergillus niger glucoamylase immobilization [7], achieving the immobilization efficiencies of 3.3-74.7% where the MCF-based glucoamylase demonstrated high performances. As described, the mesoporous silicas are mainly developed from TEOS, which is not easily found, hence a method to develop the mesoporous silicas from easily obtained materials is needed.

Bagasse bottom ash (BBA) presents a viable alternative source for the MCF silica synthesis. This worthless natural material is considered invaluable and readily available abundantly in sugarcane plants. The waste contains over 50% (w/w) SiO<sub>2</sub> [8-11], hence it must undergo the extraction and transformation process to give the MCF silica. Extraction of silica from BBA presents both economic and ecological benefits. being sustainable and environmentally friendly, while also offering the potential to decrease waste production [12-14]. This is in contrast to the silica derived from chemical precursors such as TEOS, sodium silicate, and silicic alkoxides [12]. Hermanto et al. [15] recommended enhancing process sustainability to mitigate environmental impacts, following an analysis of the life cycle assessment for a silicon production plant operating at 1 kg/h. Furthermore, transformation of the waste into amorphous nanosilica yielded a life cycle assessment indicating a global warming potential of CO<sub>2</sub> equivalent of 7.51-12.59 kg [16]. In recent investigations, mesoporous silicas were synthesized from BBA-based Na<sub>2</sub>SiO<sub>3</sub>, Pluronic P123, and surfactant in an acidic environment to adsorb dyes [17,18]. Rahman et al. [19], who compared different synthesis conditions for the mesoporous silicas derived from BBA-based Na<sub>2</sub>SiO<sub>3</sub>, revealed that the polyethylene glycolbased method produced the product having high surface area. These efforts proved the prospect of BBA to substitute TEOS.

Given the absence of methods for preparing the MCF silica from BBA, our study was conducted to explore this opportunity. In this study, potassium chloride (KCl) was employed as the expansion agent instead of TMB, aiming to lower costs associated with the MCF preparation as price of KCl is cheaper than TMB. To address the gap in research regarding immobilization of amylases on the MCF carrier as none of the amylolytic enzymes immobilizations is related to the BBA-based MCF silica as discussed previously [20], the developed salt-assisted MCF silica was used to immobilize glucoamylase. Functionality of the immobilized glucoamylase was evaluated through its application in the hydrolysis of starches.

#### 2. Materials and Methods

#### 2.1 Materials

BBA was collected from a sugarcane processing facility located in Lampung Province, Indonesia. Other materials were purchased from local suppliers: dextrose (Merck, dinitrosalicylic acid (Merck, >98%), hydrochloric acid (HCl, Merck, 37%), monobasic potassium phosphate (Merck, >99%) and monobasic sodium phosphate (Merck, >99%), sodium hydroxide (NaOH, Merck, >97%), ammonium fluoride (NH4F, Merck, >98%), potassium chloride (KCl, Merck, >99%), sodium acetate salt (Sigma, >98%), Pluronic P123 (Sigma, 435465), sulfuric acid (H2SO4, 98%), PierceTM BCA protein assay kit (Thermo Scientific), and glucoamylase. Tapioca, potato, wheat, and corn starch were bought from local supermarkets. All materials were used directly without pretreatment.

#### 2.2 Conversion of BBA to Salt-based MCF Silica

Initially, silica was obtained from the raw material. BBA was grounded and sieved to achieve the particle size of 200 mesh. 50 g of the sieved BBA was placed into a glass beaker containing 500 mL of reverse osmosis (RO) water and 5 mL of sulfuric acid. The mixture was stirred at 100 rpm for 30 minutes and then filtered. The residue was rinsed with RO water until pH of filtrate reached 7.0. The wet residue was dried at 105 °C for four hours and then calcined at 550 °C for six hours. The dried residue was transformed into sodium silicate by placing 11 g of the residue into an Erlenmeyer flask containing 50 mL of 3 M NaOH. The mixture was heated in a water bath to 80 °C for four hours, stirred at 100 rpm for 30 minutes, and then filtered to obtain the sodium silicate solution. Finally, to synthesize the BBAbased MCF silica, 4 g of Pluronic P123 was dissolved in 70 mL of 1.6 M HCl at room temperature. After incorporating 10 g of KCl into the Pluronic solution, the mixture was heated to 40 °C with vigorous stirring for two hours. Then, the sodium silicate solution was added into the mixture while maintaining high stirring speed.

The solution mixture was subsequently placed in water bath set at temperature of 40 °C for 20 Following this, the mixture was transferred to a magnetic stirrer operating at low speed, where 10 mL of ammonium fluoride at concentration of 0.92 mg.mL-1 was added gradually. An aging process was performed in water bath at 80 °C for three days. After filtration, the residue was washed with RO water until pH of filtrate was 7.0. The wet solids were dried at 100 °C for 12 h and then calcined at 300 °C for 30 minutes, followed by six hours at 500 °C to yield the BBA-based MCF silica.

# 2.3 Enzymatic Hydrolysis

To optimize adsorption of free glucoamylase the BBA-derived MCF silica, different parameters were experimented, as detailed in Table 1. Initially, free glucoamylase was introduced into 30 mL of 0.1 M Sorensen phosphate buffer. Then, 0.5 g carrier was added. The mixture was put into water bath shaker, maintained at certain speed and temperature. After five hours, the mixture was filtered. The residue was washed with 0.1 M Sorensen buffer (3×50 mL) in accordance with pH of the immobilization process. Filtrates from separation and washing stage were stored in refrigerator prior to protein analysis. The wet residue was dried overnight in oven set at 40 °C and then allowed to cool. The dried product was kept in refrigerator before used. Efficiency of the immobilization process was based-on the difference between the initial and concentration of free enzyme as described in the previous literatures [1-3].

Performance of the immobilized glucoamylase in hydrolysis of starches was assessed based-on the operating conditions as shown in Table 1. The procedure began with addition of 30 mL of a 0.1 M sodium acetate buffer into a 100 mL Erlenmeyer flask. After that, a specific concentration of starch was introduced into the medium. The immobilized glucoamylase was mixed with the starch solution. The mixture was agitated in a water bath shaker at a certain speed and temperature for eight hours. Samples were collected at the beginning and end of the process. Hydrolysis using free

glucoamylase was also performed under identical conditions to facilitate comparison of the enzyme activity.

#### 2.4 Reusability Study

The immobilized glucoamylase was used repeatedly in a batch reactor where the operating conditions were based-on the optimum hydrolysis operational factors. It was set as follow: the optimum amount of starch was dissolved in a 100 mL Erlenmeyer flask containing 30 mL of 0.1 M sodium acetate buffer at its optimum pH. Then, glucoamylase was immobilized according to the optimum initial enzyme concentration. The mixture was placed in a water bath shaker set at its optimum agitation speed for The initial dan final samples were 8 hours. collected for DE analysis. After the hydrolysis process, the immobilized enzyme was filtered-off and washed with 0.1 M sodium acetate buffer at the optimum pH (3×50 mL). The residue was reintroduced into a fresh reaction medium and its performance checked. The immobilized enzyme activity was determined to be 100% in the 1st trial. Activities obtained in other runs were compared with that of the 1st trial.

# 2.5 Characterizations and Analysis

The nitrogen adsorption-desorption isotherm data were collected using a Quanta-chrome NOVA touch LX-4 automated gas sorption analyzer operated at liquid nitrogen temperature, to estimate the average cell pore size, average window pore size, specific pore volume, and specific surface area using the Barrett-Joyner-Halenda (BJH) method and the Brunauer-Emmett-Teller (BET) method. Samples of the carrier and immobilized enzyme were also analyzed through the Agilent FTIR spectroscopy. Protein content was determined using PierceTM BCA protein assay kit, while hydrolysis of starches was assessed by the DNS method. A Shimadzu UV-VIS 1800 spectrometer was employed to quantify the protein and glucose levels.

Table 1. The operational factors of immobilization and hydrolysis process.

Evenouismental Factor	Enzyme	Starch	
Experimental Factor	Immobilization <sup>2</sup>	${ m Hydrolysis}^2$	
Enzyme concentration	$2\text{-}10~\mathrm{mg.mL^{-1}}$	2,500-10,000 U	
Agitation speed	80-140 rpm	120-160 rpm	
Sorensen buffer pH	5.0-7.0	4.1-5.1	
Temperature	30-50 °C	40-80 °C	
Starch concentration		3-8% (w/v)	

#### 3. Results and Discussion

The immobilization of free glucoamylase to the MCF silica carrier derived from BBA was achieved through adsorption. The process involved submerging the carrier in an enzyme solution for a certain time under conditions that maintain the activity of glucoamylase, as described in Figure 1. The physical attachment of the enzyme to the carrier was facilitated by noncovalent interactions, such as the electrostatic attraction between oppositely charged entities or hydrogen bonding. Although this method is straightforward and economical, it results in enzyme leaching due to the relatively weak interactions between the enzyme and the carrier [21-23].

The MCF silica is synthesized from inorganic silica species through formation of hydrogen bonds, as indicated in reference [24]. This process involves the addition of an expansion agent, which facilitates the transition from a highly ordered hexagonal symmetry to the MCF structure [25]. In our experimental procedure, KCl was employed as the expansion agent, following recommendation by Choi et al. [26]. The synthesis was conducted under acidic conditions using HCl, where assembly of the hydrophilic group and positively charged silica species occurred through electrostatic interactions, which were mediated by negatively charged chloride ions.

The surface area, pore volume, and pore size after the BJH desorption analysis are presented in Table 2. The BBA-MCF silica carrier exhibited a surface area of 48.5 m<sup>2</sup>.g<sup>-1</sup>. The diameters of the

carrier pores were distributed between 3.05 and 26.32 nm, with a peak diameter observed at 9.33 nm. The BJH desorption cumulative micropore volume measured 0.1214 cm<sup>3</sup>.g<sup>-1</sup>. The distribution of the carrier pore was identified within the range of 0.003-0.017 cm<sup>3</sup>.nm<sup>-1</sup>.g<sup>-1</sup>, where 46.24% of the pore volume consisted of the carrier pore diameters exceeding 6 nm. These characteristics are smaller than the TEOS-TMB-derived MCF silica, which, for example, has BET surface area of 378 m<sup>2</sup>.g<sup>-1</sup>, pore volume of 2.12 cm<sup>3</sup>.g<sup>-1</sup>, and pore diameter size of 15.8 nm [1,2,27]. Additionally, the MCF silica developed by Choi et al. [26] from KCl salt and Aldrich sodium silicate solution had high surface area (309-387 m2.g1) and pore volume (1.28-1.56 cm<sup>3</sup>.g<sup>-1</sup>), but with similar pore diameter sizes (9.07-13.7 nm). It seems that the MCF silica prepared using KCl salt resulted in smaller pore sizes compared to the one derived from trimethylbenzene (TMB). TMB is a bulky organic compound and known as expanding/swelling agent capable of enlarging micelles or creating significant voids within the precursor structure [28,29], while KCl is a crystalline inorganic salt that typically produces small and less adaptable templates, leading to the development of small pores [30,31]. In the preparation stage, our research used 10 g of KCl along with diluted HCl, contrasting notably with the approach taken by Choi et al. [26] who used 5 g of KCl and diluted acetic acid for formation of the carrier from Aldrich sodium silicate. Hence, further observations are required in development of salt-assisted MCF silica from BBA to increase

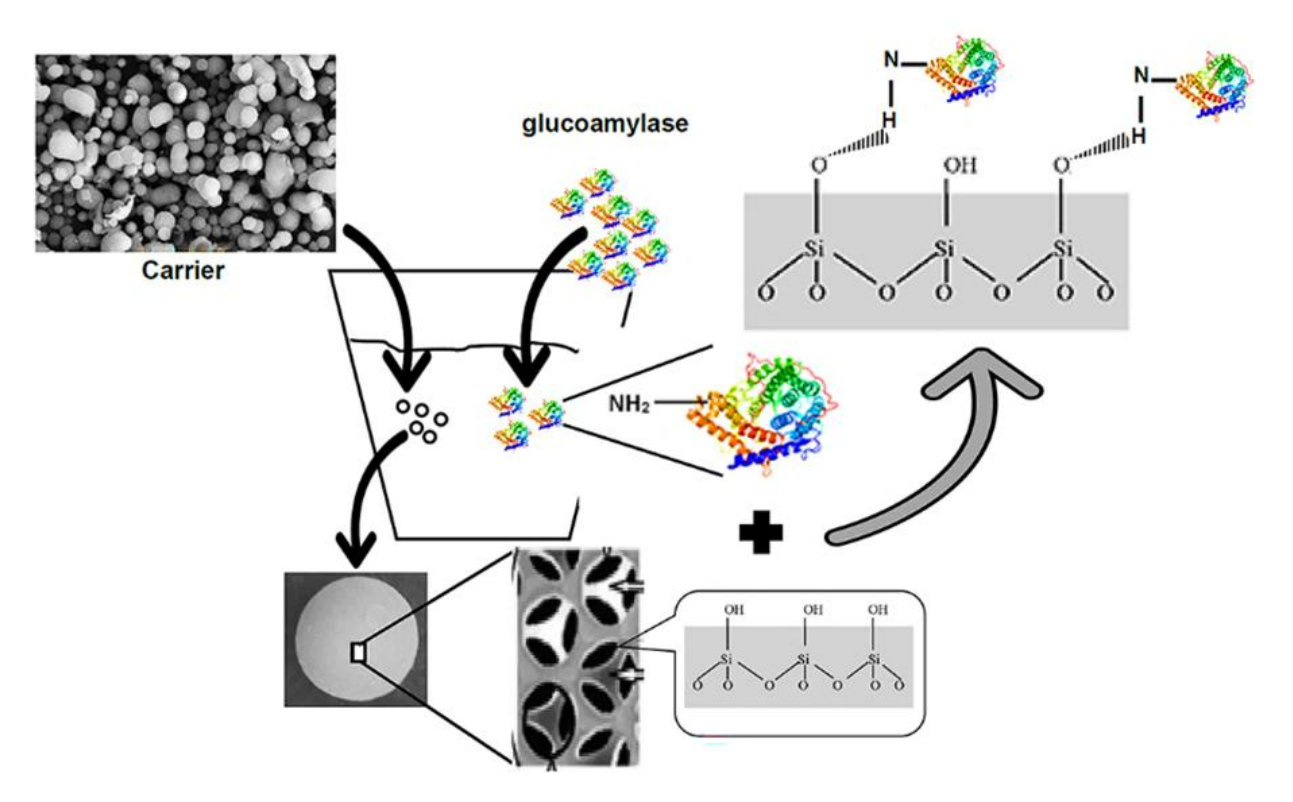


Figure 1. Adsorption of glucoamylase to the BBA-derived MCF silica.

surface area of the product, such as optimization of the salt concentration and revision of the preparation method. Choi *et al.* [26] who prepared the S-MCF from Aldrich sodium silicate concluded that the surface area and pore volume of the silica decreased in the presence of higher concentrations of salts in the synthetic solution.

Mesoporous properties of the BBA-derived MCF silica were evaluated through the N<sub>2</sub> adsorption-desorption isotherms and pore-size distribution, as shown in Figure 2. The observed hysteresis loop was characteristic of mesoporous silica materials, classified as type IV [32,33], typical of materials with mesoporous channels and cavities. The hysteresis was noted in the relative pressure (P/P<sub>0</sub>) range of 0.5 to 0.94, confirming presence of mesostructured pores. As described previously, the pore sizes of the carrier were distributed between 3.05 and 26.32 nm, with peak diameter of 9.33 nm. After glucoamylase immobilization, there was a significant reduction in pore volume and average diameter to 3.4 nm, indicating that the enzyme occupied the pores. This reduction can be attributed to three main factors: size of the enzyme, which blocks the larger pores; electrostatic interactions between the functional groups of the enzyme and the silica pore walls, favoring immobilization; and the synthesis conditions, such as presence of KCl, which may have influenced the final structure of the material, reducing the available surface area after immobilization. Thus, the observed reduction in surface area and pore volume reflects the efficient immobilization of glucoamylase, as confirmed by the isotherms and pore distribution.

The FTIR analysis is shown in Figure 3. Strong vibrations occurred in the wavelength range of 1,300-850 cm<sup>-1</sup>, peaking at 1,013.8 cm<sup>-1</sup>. Literatures indicated that these frequencies related with the silicone-oxy compounds (Si-O-Si group) [32,33]. A medium peak was observed at 1,640 cm<sup>-1</sup>. This peak belongs to the double bond region [32] and could associate with the following functional groups: C=C stretching, primary amine (N-H bend), secondary amine (>N-H bend, C=O stretching), amide (NH2 bending, C=O stretch), and organic nitrates [34-37]. A strong vibration peak was found at 3,347.1 cm<sup>-1</sup>. The peak existed in the single bond region [33] and related to the following functional groups: hydroxyl group (Hbonded, OH stretch), primary amide (NH<sub>2</sub> stretch), secondary amine (>N-NH-stretch), Si-OH stretch [34-37]. These vibrations were related

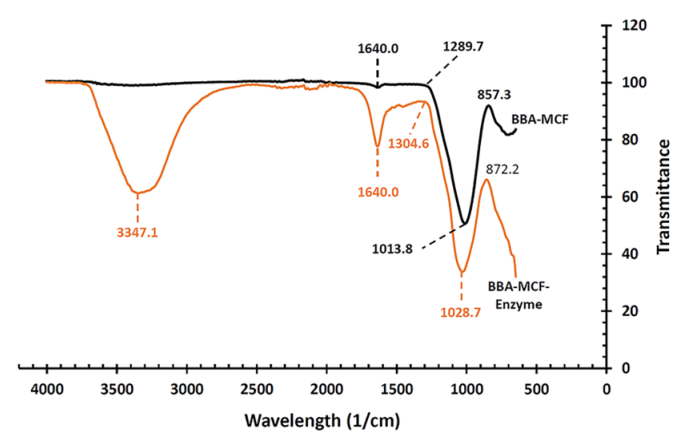


Figure 3. FTIR spectrum of the carrier and immobilized enzyme

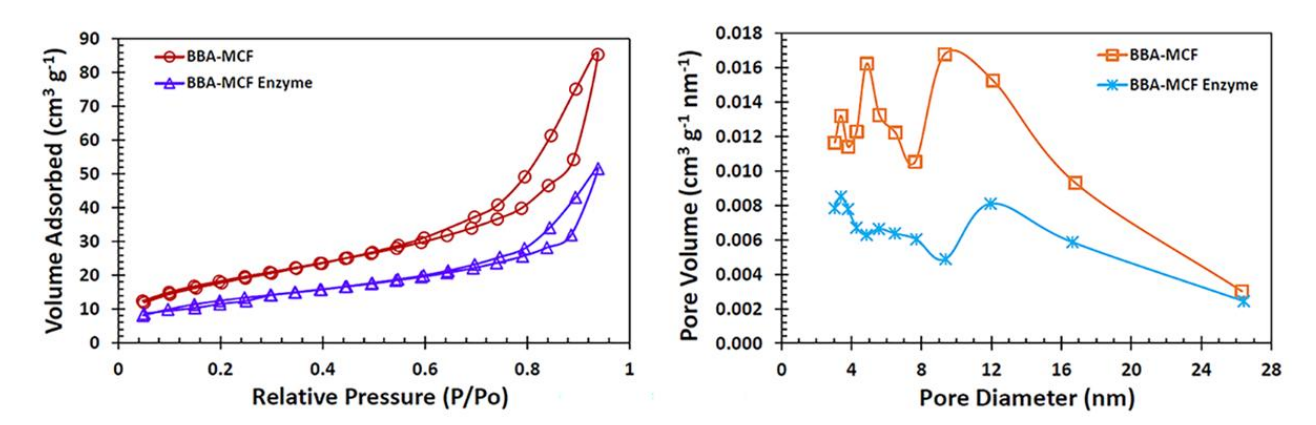


Figure 2. N<sub>2</sub> adsorption-desorption isotherms (left) and pore size distribution (right) of the BBA-based MCF silica and immobilized glucoamylase.

Table 2. BJH desorption of the carrier and immobilized enzyme.

Compound	Surface Area (m².g <sup>-1</sup> )	Micropore Volume (cm³.g·1)	Pore Diameter (nm)	
BBA-MCF Silica	48.5	0.12	9.33	
BBA-MCF Silica-Enzyme	26.3	0.07	3.4	

with glucoamylase since the enzyme is composed by amino acid compounds, which basically contain amino groups (-NH<sub>2</sub>) and carboxyl groups (-COOH). The observed frequencies were slightly lower than those observed in the TEOS-based MCF silica as described previously [1-3].

Figure 4 indicates that the BBA-derived MCF silica contains a significant amount of silicon (Si) compound even though the initial silica (SiO<sub>2</sub>) content in the BBA extract was quite high (96.46% (w/w)) found after the gravimetric analysis. However, following the pre-treatment process, the extracted BBA retained only trace amounts of aluminum (Al). The SEM-EDX analysis suggests that the minimal presence of aluminum could contribute to the aggregation of BBA-based MCF silica. Furthermore, presence of carbon (C), oxygen (O), and silicon (Si) elements in the immobilized enzyme sample confirms that these elements are associated with both the carrier material and the chemical composition of the enzyme. Carbon, oxygen, and nitrogen, in particular, are indicators of $_{
m the}$ organic components contributed by the glucoamylase enzvme.

Adsorption of free glucoamylase onto the carrier was further confirmed by reduction in pore diameter (Table 2). The pore size decreased to 3.4 nm, suggesting that the enzyme molecules occupied the carrier's surfaces. The salt-assisted BBA-based MCF silica proved to be effective for glucoamylase adsorption, accommodating enzymes with molecular weights of less than 200 kDa (~ 80 Å), such as *Aspergillus terreus* 

glucoamylase (86 kDa) [38]. Aspergillus niger glucoamylase (46-118 kDa) [39,40], Thermomyces lanuginosus glucoamylase (52-72 kDa) [41,42], and Amylomyces sp. glucoamylase [43]. George et al. [6] noted that the mesoporous silica channels were specifically designed to accommodate enzyme molecules with dimensions similar to glucoamylase's.

The  $N_2$ adsorption-desorption isotherm (Figure 2) confirmed the immobilization, as the hysteresis loop for the immobilized enzyme shifted between 0.64-0.94. The significant decrease in the pore volume after the enzyme attachment confirmed the reduction in available pores, further supporting efficient adsorption onto the salt-assisted BBA-based MCF silica. Despite the reduction in pore volume, the overall mesoporous structure of the material remained intact after enzyme immobilization, as evidenced by the preserved adsorption-desorption profile. Additionally, the FTIR analysis (Figure 2) provided further validation for glucoamylase adsorption. The peaks related to Si-O-Si stretching at 1,028.7 cm<sup>-1</sup> remained present, while new peaks, especially at 1,640.0 cm<sup>-1</sup> and 3,347.1 cm<sup>-1</sup>, were identified, corresponding to amide and amine bonds from the enzyme's polypeptide chain [2,36,44].

Results of the enzyme adsorption onto carrier are illustrated in Figure 5. Four factors, i.e. free enzyme concentration, agitation speed, Sorensen buffer pH, and temperature, were analyzed using the OFAT approach. Overall, the immobilization efficiencies ranged from 78.0% to 88.5%, with the

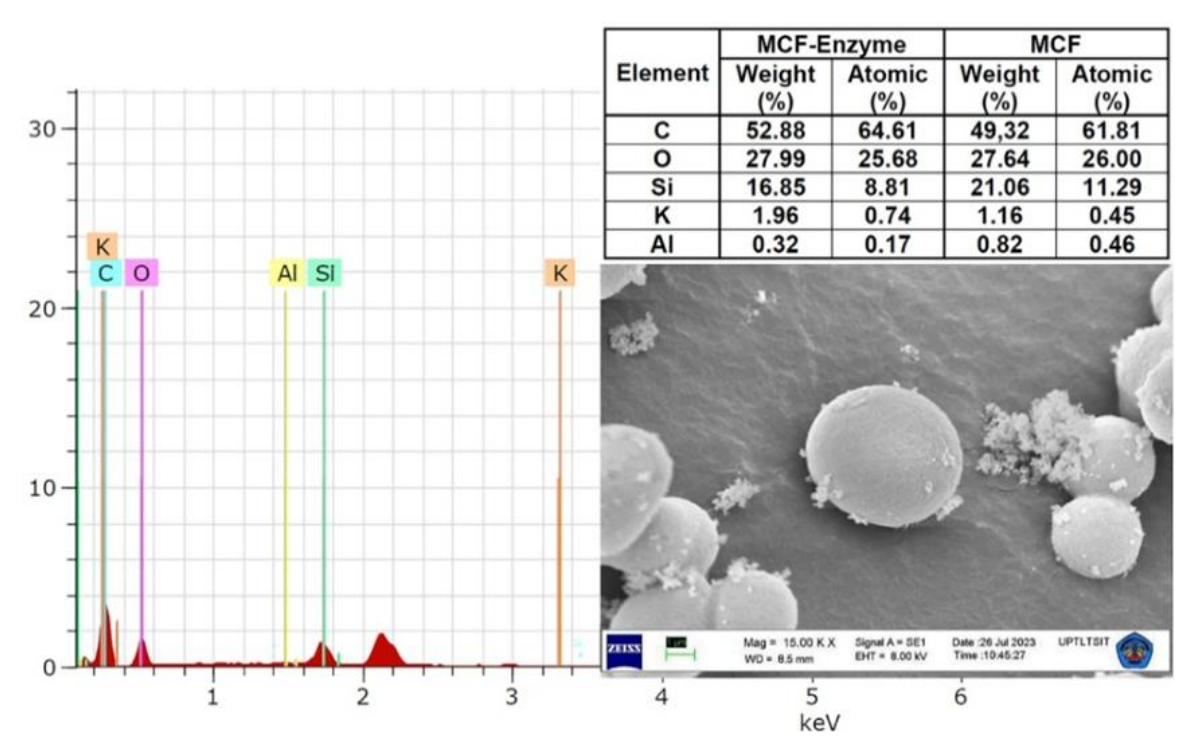


Figure 4. SEM-EDX on the immobilized glucoamylase (Carbon (C), Oxygen (O), Silicone (Si), Aluminum (Al), Potassium (K)).

highest efficiency achieved at the optimal operational temperature, while the lowest enzyme concentration yielded the least favorable results. The optimal parameters identified were an enzyme concentration of 9.0 mg.mL<sup>1</sup>, an agitation speed of 120 rpm, a buffer pH of 5.5, and an operational temperature of 30 °C.

The immobilization temperature was examined in the range of 30-50 °C. The highest efficiency, approximately 88.5%, was recorded at 30 °C, while the lowest result, around 82.0%, was observed at 50 °C (uncertainty analysis: average value = 85.6%, confidence interval at 95% confidence level = 2.00). At 35 °C, immobilization efficiency approached the optimal level, with only a minor difference in efficiency (< that the immobilization 2%), suggesting temperature could be fine-tuned within the 30-35 °C range. Beyond 45 °C, a significant decline in immobilization efficiency was noted, exceeding 3%. The factor demonstrated a significant impact on the immobilization process, as indicated by the regression analysis, which yielded a coefficient of determination  $(R^2)$  of 0.93 along with a low significance F and p-value (< 0.05). The optimal temperature identified in these experiments aligned with findings from a previous study that utilized TEOS-based MCF silica as a carrier for glucoamylase [2]. However, the immobilization of glucoamylase on the salt-assisted BBA-based MCF silica yielded a slightly higher efficiency (approximately 3%). Previous studies reported achieving the optimal immobilization efficiencies at 30 °C [6,45]. Conversely, Aspergillus niger glucoamylase was immobilized on various mesoporous silicas primarily derived from TEOS conducted at the ambient temperature [4].

pH of a 0.1 M Sorensen phosphate buffer was adjusted between 5.0 and 7.0, found significantly influencing the process. Generally, an increase in

the pH of the medium results in a decrease in immobilization efficiency. The immobilization efficiency was recorded at pH of 5.5, with approximately 88.5% of the free enzyme being immobilized, while the lowest efficiency, around 78%, was observed at pH of 7.0 (uncertainty analysis: average value = 83.3%, confidence interval at 95% confidence level = 4.01). The substantial difference between these two conditions underscores the significant impact Sorensen buffer pH on glucoamylase immobilization. Similar to the preceding factor, the pH of buffer exhibited a significant impact, as indicated by the  $R^2$  value of 0.90, with both the significance F and p-value were below 0.05. The optimal buffer pH aligns with previous findings regarding the immobilization of glucoamylase on TEOS-based MCF silica [2].

Impact of free glucoamylase concentration was examined in the range of 5-10 mg of enzyme per mL of buffer. The highest efficiency achieved was approximately 88.5% at the concentration of 9.0 mg.mL<sup>-1</sup> (equivalent to 270 g of free enzyme), while the lowest efficiency recorded was 78% at the minimum concentration of 5.0 mg.mL<sup>-1</sup> (uncertainty analysis: average value = 83.8 %, confidence interval at 95% confidence level = 3.22). The initial enzyme concentration was found have substantial impact а on immobilization process, as evidenced by the significant disparity between the maximum and minimum immobilization efficiencies. Examination of the efficiency data via regression analysis revealed a notably high  $R^2$  value of 0.761, accompanied by a low significance F and p-value, both of which are less than 0.05. In comparison to TEOS-based MCF silica [2,7], a greater quantity of glucoamylase was immobilized on the BBAbased MCF silica, indicating a higher availability of enzymes on the surfaces of the BBA-based

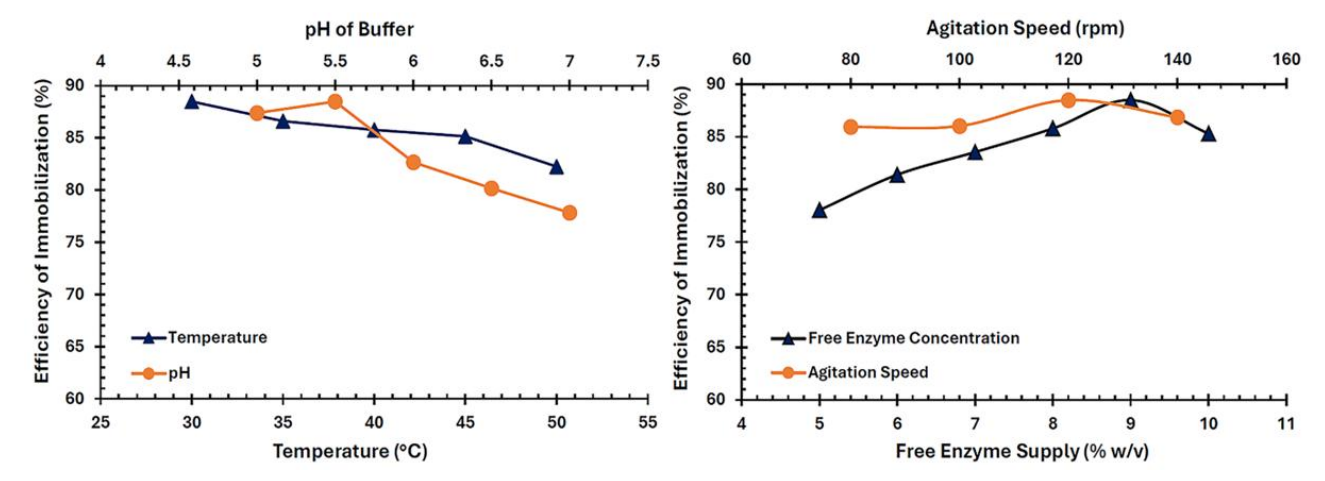


Figure 5. Effects of the operational factors on immobilization ([factors constant at temperature variation: 120 rpm, 270 mg free enzyme; pH of 5.5]; [factors constant at buffer pH variation: 120 rpm, 270 mg free enzyme, 30 °C]; [factors constant at enzyme concentration variation: 120 rpm, pH of 5.5, 30 °C]; [factors constant at agitation speed variation: 270 mg free enzyme, 30 °C, pH of 5.5])

carrier. Bayne *et al.* [46] noted that carriers with pore sizes of 10-100 nm exhibited reduced protein loads as pore size increased.

Agitation speed of the mixture was varied between 80 and 140 rpm. The maximum efficiency recorded was 88.5% at 120 rpm, while the minimum efficiency of 86% occurred at 80 rpm (uncertainty analysis: average 86.8%, confidence interval at 95% confidence level = 1.16). This parameter had a negligible impact on the immobilization process, given the small difference between the highest and lowest efficiencies. The regression analysis showed a low  $R^2$  of 0.32; however, the significance F was notably high at 0.43, despite the p-value was less than 0.05. Previous studies indicated that a lower speed of 100 rpm achieved agitation glucoamylase immobilization efficiency of 84.8% on TEOS-based MCF silica, despite utilizing the amount of MCF silica [2].niger immobilization of free Aspergillus glucoamylase on amino-functionalized TEOSbased large ordered mesoporous silica carriers, a higher agitation speed of 200 rpm was employed [4,6].

The specific activities of both free and immobilized glucoamylase were evaluated using soluble starch in 0.30 L of 0.05 M sodium acetate buffer at a pH of 4.5. The analysis revealed that the immobilized enzyme exhibited a slightly lower specific activity compared to its counterpart (Figure 6). Specifically, the specific activities for free and immobilized glucoamylase were recorded at 23,848 U.g-1 and 20,578 U.g-1, respectively. These reductions could be caused conformational changes on the enzyme structures during the immobilization process as some enzyme active sites are difficult to be accessed by the substrate [47,48]. Milosevic et al. [49,50] explained the diffusional limitations had occurred caused by the support that reduces the access of the substrate to the active sites of the bound enzyme. Further, Milosevic et al. [51] concluded the immobilization process interferes with the enzyme catalytic site and/or by diffusional problems generally produced when immobilized

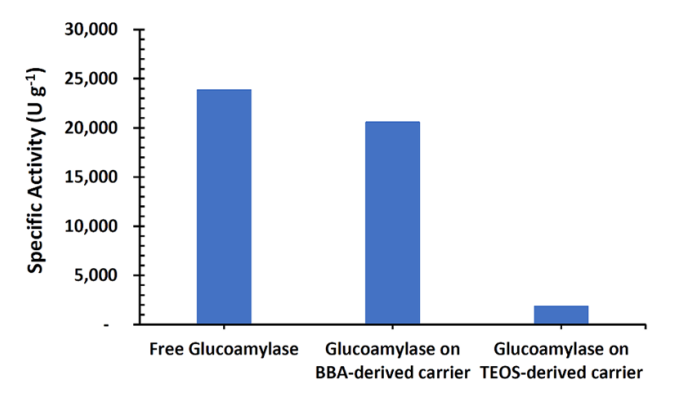


Figure 6. The comparison of enzyme specific activity.

enzvmes are acting on macromolecular substrates. The obtained specific activity surpassed the specific activity of glucoamylase immobilized on TEOS-based MCF silica, which was measured at 1,856.78 U.g-1 [2]. Additionally, the specific activities from the immobilization of glucoamvlase on functionalized nanoparticles, mesoporous carbon, and poly(CMAco-EGDMA) were lower, yielding 1,408.6 U.g-1 [52], 84-540 U.g<sup>-1</sup> [50,51], and 700-1,100 U.g<sup>-1</sup> [49,51], respectively. It is common for the activity of free enzymes to diminish when glucoamylase is immobilized on inorganic carriers; for instance, glucoamylase immobilized on Sibunit retained less than 20% of the activity of free glucoamylase [53,54]. Moreover, immobilization on polymeric compounds often resulted in even lower specific activities, typically below 10% [49-51]. However, a notable increase in specific activity, reaching up to 55%, was observed when free glucoamylase was immobilized in magnetic clays [55].

Hydrolysis of starches, including tapioca, wheat, potato, and corn, were subjected to variations through the operational experiments over a duration of eight hours in 30 mL of 0.1 M sodium acetate buffer. The processes yielded low to moderate Dextrose Equivalent (DE) values; however, the free glucoamylase exhibited higher DE values compared to the immobilized enzyme, as shown in Table 3. Previous studies demonstrated that the free Sigma-Aldrich Aspergillus niger glucoamylase activity was enhanced through its adsorption and covalent bonds onto TEOS-based mesoporous silicas [4]. In contrast, the Gist-Brokades glucoamylase (Amigase, batch 8187/SPE 0551) immobilized on the TEOS-based MCF silicas via adsorption and covalent bonds gave products with greater activity than the free glucoamylase, with the unique pore structure of the MCF playing a pivotal role in the enzyme immobilization [7]. Additionally, the hydrolysis of tapioca starch using glucoamylase immobilized on TEOS-based MCF silica achieved a maximum DE value of 76.3% at a temperature of 70 °C, a buffer pH of 4.1, and an agitation speed of 140 rpm. In starch hydrolysis processes, the immobilization of Sigma-Aldrich Aspergillus niger glucoamylase on mesoporous silica through adsorption or covalent bonding enhances the enzyme's stability and results in products with higher catalytic activity compared to free glucoamylase [6].

Activity of the immobilized glucoamylase was found to be lower than that of the free enzyme during variation of the sodium acetate buffer pH, which exhibited peak activity at pH of 4.6, whereas the immobilized enzyme demonstrated optimal performance at pH of 4.1. The DE values for the immobilized glucoamylase throughout the experiments ranged from 8.1% to 45.6% (uncertainty analysis: average value = 29.69)

(tapioca), 11.13 (potato), 15.55 (corn), 10.76 (wheat), confidence interval at 95% confidence level = 5.58 (tapioca), 15.96 (corn), 6.39 (wheat), 3.56 (potato)), with hydrolysis of tapioca and corn starch yielding superior DE results. In contrast, the free enzyme achieved DE values as high as 65% during the hydrolysis of corn (uncertainty analysis: average value = 39.96 (tapioca), 14.79 (potato), 58.51 (corn), 15.59 (wheat), confidence interval at 95% confidence level = 4.24 (tapioca), 48.49 (corn), 6.69 (wheat), 5.43 (potato)). A significant disparity in enzyme activities was noted in the hydrolysis of corn; however, both enzymes displayed minimal DE differences when hydrolyzing tapioca, wheat, and potato starch. The small variation between the maximum and minimum DE values suggests a limited impact of this factor on the performance of the immobilized enzyme during starch hydrolysis. A similar optimal pH was observed in the hydrolysis of tapioca using glucoamylase adsorbed on the In contrast, TEOS-based MCF silica [2]. covalently bonded glucoamylase on certain silicas mesoporous demonstrated optimal hydrolysis of a 3% (w/v) starch solution at a higher pH range of 5.0 to 6.0 [6].

The operational temperature for the hydrolysis process was adjusted within the range of 40-80 °C. Similar to the buffer pH, activity of the immobilized glucoamylase remained lower than that of the free enzyme. Both enzyme types exhibited the same optimal temperature. The derived DE values reached as high as 35.4% for the immobilized enzyme (uncertainty analysis: average value = 27.50 (tapioca), 11.20 (potato), 19.52 (corn), 13.20 (wheat), confidence interval at 95% confidence level = 8.23 (tapioca), 8.80 (corn),

5.66 (wheat), 2.99 (potato)) and up to 79.1% for the free glucoamylase (uncertainty analysis: average value = 33.09 (tapioca), 13.45 (potato), 56.97 (corn), 21.82 (wheat), confidence interval at 95% confidence level = 12.46 (tapioca), 16.86 (corn), 5.38 (wheat), 2.68 (potato)), with both potato and tapioca starch hydrolysis yielding comparable DE values for each enzyme. When varying this factor, the hydrolysis of tapioca and corn starch resulted in superior DE values compared to other starches. The factor significantly influenced the hydrolysis process, as evidenced by the minimal difference between the highest and lowest DE values produced by the immobilized glucoamylase. During the hydrolysis, the optimal temperature varied considerably among the starches. The hydrolysis of tapioca and corn starch using the immobilized glucoamylase was optimal at 50 °C, whereas the hydrolysis of wheat and potato starch required higher optimal temperatures of 60 °C and 70 °C, respectively. Previous studies indicated that the effect of process temperature on the activity ofimmobilized Aspergillus glucoamylase in starch hydrolysis within the same buffer was optimal at temperatures ranging from 30-40 °C [6]. However, Zhao et al. [56] demonstrated that the immobilized Aspergillus niger glucoamylase exhibited higher optimal temperatures, specifically between 55-65 °C, compared to the free glucoamylase in the soluble starch hydrolysis process.

Additional operational parameters, including the initial concentration of enzyme, starch concentration, and agitation speed, were also varied to assess their impacts. Performance of the immobilized glucoamylase remained inferior to that of the free enzyme, consistent with the

m 11 o	TOTAL	1	c		. 1	1 1	1 .
Table 3.	1 ) H;	values	Ωt	Various	starch	hvdi	rolvsis
Table 6.	$\boldsymbol{\nu}$	varacs	OI	various	Starti	my cm	cory oro.

Factor	Wheat		Corn		Potato		Tapioca	
ractor	Free	Adsorbed	Free	Adsorbed	Free	Adsorbed	Free	Adsorbed
Buffer pH	10.2-21.9	8.1-17.2	40.4-65.0	37.9-45.6	9.5-18.8	8.9-14.7	36.1-43.6	26.7-35.4
Temperature	13.2-40.7	5.1-25.0	42.9-79.1	10.7-31.8	9.6-16.0	7.8-14.7	26.8-40.2	23.1-35.4
Enzyme Concentration	20.8-43.0	17.3-34.5	7.4-79.1	5.6-31.8	16.9-24.4	12.2-19.5	23.3-42.5	21.6-35.4
Starch Concentration	20.9-45.4	25.9-32.2	35.6-87.8	12.1-49.1	24.4-38.3	14.3-52.9	17.6-38.3	19.1-45.6
Agitation Speed	27.1-46.4	14.8-29.9	13.6-87.8	7.1-49.1	24.6-46.8	43.4-63.9	40.4-65.0	37.9-45.6
Optimum pH	4.6		4.1	4.6	4.1	4.6	4.1	4.6
Optimum Temperature	60 °C		50 °C		70 °C		50 °C	
Optimum [Enzyme]	7500 U		5000 U		7500 U		5000 U	
Optimum [Starch]	5 mg.mL <sup>-1</sup>		$2 \text{ mg.mL}^{-1}$		$3 \text{ mg.mL}^{-1}$		5 mg.mL <sup>-1</sup>	$3 \text{ mg.mL}^{-1}$
Optimum Speed	140 rpm		140 rpm		120 rpm	160 rpm	120 rpm	140 rpm

OFAT Design: *1*) Effect of buffer pH (tapioca: 50 °C, 140 rpm; 5% (w/v) starch, 5,000 U enzyme; potato: 70 °C, 140 rpm; 5% (w/v) starch, 5,000 U enzyme; corn: 50 °C, 140 rpm; 4% (w/v) starch, 5,000 U enzyme); wheat: 60 °C, 140 rpm; 5% (w/v) starch, 5,000 U enzyme); *2*) Effect of temperature (tapioca, wheat & potato: pH 4.6, 140 rpm, 5% (w/v) starch, 5,000 U enzyme; corn: pH 4.6, 140 rpm, 4% (w/v) starch, 5,000 U enzyme); *3*) Effect of free enzyme concentration (tapioca: 50 °C, pH 4.6, 140 rpm, 5% (w/v) starch; wheat: 60 °C, pH 4.6, 140 rpm, 5% (w/v) starch; potato: 70 °C, pH 4.6, 140 rpm, 5% (w/v) starch; corn: 50 °C, pH 4.6, 140 rpm, 4% (w/v) starch); *4*) Effect of starch concentration (tapioca, corn: 50 °C, pH 4.6, 140 rpm, 5,000 U enzyme; wheat: 60 °C, pH 4.6, 140 rpm, 7,500 U enzyme; potato: 70 °C, pH 4.6, 140 rpm, 7,500 U enzyme; b) Effect of agitation speed (tapioca: 50 °C, pH 4.6, 3% (w/v) starch, 5,000 U enzyme; wheat: 60 °C, pH 4.6, 5% (w/v) starch, 7,500 U enzyme; potato: 70 °C, pH 4.6, 3% (w/v) starch, 7,500 U enzyme; corn: 50 °C, pH 4.6, 2% (w/v) starch, 5,000 U enzyme)

findings of the previous two factors, where the produced DE ranged from 7.1% to 63.9% for the enzyme (uncertainty analysis: immobilized average value = 28.62-41.06 (tapioca), 16.13-54.00(potato), 18.08-36.44 (corn), 22-55-28.29 (wheat), confidence interval at 95% confidence level = 3.74-15.08 (tapioca), 13.47-23.89 (corn), 3.88-8.56 (wheat), 4.12-9.92 (potato)) and from 7.4% to 87.8% for the free enzyme (uncertainty analysis: average value = 29.22-53.39 (tapioca), 20.83-36.58 (potato), 35.19-65.50 (corn), 29.62-34.32 (wheat), confidence interval at 95% confidence level = 8.78-12.60 (tapioca), 31.66-43.11 (corn), 3.88-15.51 (wheat), 3.88-12.81 (potato)). The optimal initial enzyme concentrations were determined to be 5,000 U for corn and tapioca, and 7,500 U for wheat and potato. Starch sources such as potato, corn, and tapioca yielded superior results compared to wheat starch. The influence of starch concentration on the hydrolysis process was found to be optimal within the range of 2-5 mg.mL<sup>-1</sup>. The ideal agitation speed for hydrolysis processes utilizing immobilized glucoamylase was identified as 140 rpm, with the exception of potato starch hydrolysis, which exhibited performance nearly equivalent to that of free glucoamylase. The agitation factor was deemed to have a minimal effect on the hydrolysis process. Notably, variations in agitation speed led to increased DE values in potato starch hydrolysis when employing immobilized glucoamylase compared to the free enzyme.

Reusability on an immobilized enzyme is considered a must for large-scale operations [57]. Hence, the repeated uses of the immobilized glucoamylase were studied to observe its capability after many hydrolysis cycles of tapioca and potato starch (Figure 7). In general, the immobilized enzyme still showed activity of more than 50% after 4 (four) cycles. The results did not differ greatly with the TEOS-based MCF silica that reached > 50% after 5 (five) cycles [1]. Reductions of the immobilized glucoamylase activity could occur as it must be washed several

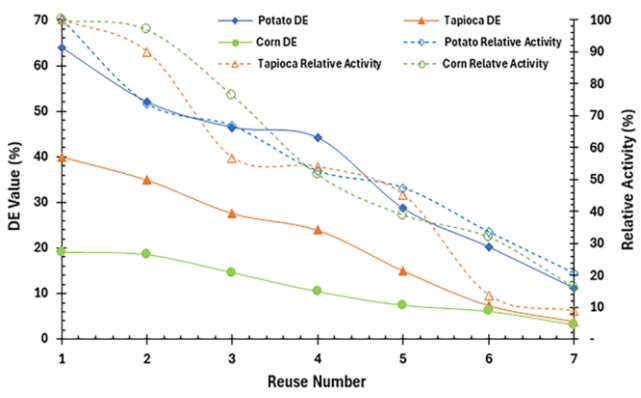


Figure 7. Reusability of the immobilized glucoamylase.

times with the buffer solutions that caused the enzyme leaching from the carrier [58,59].

#### 4. Conclusion

The use of bagasse boiler bottom ash (BBA) has proven to be a sustainable and efficient alternative for synthesis ofsalt-assisted mesoporous MCF silica. The carrier demonstrated favorable characteristics for glucoamylase immobilization, including a good surface area and adequate pores, confirming the potential of BBA as a raw material source for these processes. Enzyme immobilization occurred effectively, with significant yield, especially under optimized conditions ofenzyme concentration, temperature, and agitation speed. The results highlighted that, although the specific activity of the immobilized enzyme was slightly lower than that of the free enzyme, the immobilization process provided greater stability and consistent performance throughout the hydrolysis of different starches. This reinforces the viability of using supports derived from agro-industrial waste for biotechnological applications. Therefore, this study paves the way for the development of more sustainable industrial processes by converting natural waste into functional materials for biocatalysis. BBA-derived MCF silica, with its favorable properties and promising performance in enzyme immobilization, can be applied in various industrial contexts, especially in starch hydrolysis and potentially in other enzymatic biotransformations.

### **Declaration of AI Technology**

We declare that no Artificial Intelligence (AI) technologies or AI-assisted tools were utilized in any capacity during the writing and preparation of this article.

#### **Conflict of Interest**

No conflict of interest was declared by the authors.

### Acknowledgments

All authors express their gratitude to Directorate General of Higher Education, Ministry of Education and Culture of Republic of Indonesia, for providing financial support in 2023 through The National Basic Research Grant (No. 2192/UN26.21/PN/2023).

### **CRedit Author Statement**

Author Contributions: J. Agustian: Conceptualization; Data curation; Formal analysis; Funding acquisition; Investigation; Methodology; Project administration; Resources;

Supervision; Validation; Visualization; Roles/Writing - original draft; Writing - review & editing; L. Hermida: Conceptualization; Data curation; Investigation; Methodology; Supervision; Validation; Roles/Writing - original draft; Writing - review & editing. All authors have read and agreed to the published version of the manuscript.

#### References

- [1] Agustian, J., Hermida, L. (2018). Saccharification kinetics at optimized conditions of tapioca by glucoamylase immobilized on mesostructured cellular foam silica. *Eurasian Chem. Technol. J.* 20, 311-318. DOI: 10.18321/ectj764
- [2] Agustian, J., Hermida, L. (2019). Capability of immobilized glucoamylase on mesostructured cellular foam silica to hydrolyze tapioca starch. *Mater. Sci. Eng.* 509, e012058. https://iopscience.iop.org/article/Mater.Sci.Eng1 0.1088/1757-899X/509/1/012058/pdf
- [3] Agustian, J., Hermida, L. (2019). The optimized statistical model for enzymatic hydrolysis of tapioca by glucoamylase immobilized on mesostructured cellular foam silica. *Bull. Chem. React. Eng. Catal.* 14, 380-390. DOI: 10.9767/bcrec.14.2.3078.380-390
- [4] George, R., Sugunan, S., (2014). Kinetic and thermodynamic parameters of immobilized glucoamylase on different mesoporous silica for starch hydrolysis: A comparative study. J. Mol. Catal. B: Enzymatic 106, 81-89. DOI: 10.1016/j.molcatb.2014.04.016
- [5] Vlad-Oros, B., Preda, G., Dudas, Z., Dragomirescu, M., Chiriac, A. (2007). Entrapment of glucoamylase by sol-gel technique in PhTES/TEOS hybrid matrixes. Process Appl. Ceramics 1, 63-67. DOI: 10.2298/PAC0702063V
- [6] George, R., Gopinath, S., Sugunan, S. (2013). Improved stabilities of immobilized glucoamylase on functionalized mesoporous silica synthesized using decane as swelling agent. Bull. Chem. React. Eng. Catal. 8, 70-76. DOI: 10.9767/bcrec.8.1.4208.70-76
- [7] Szymanska, K., Bryjak, J., Mrowiec-Białon, J., Jarzebski, A.B. (2007). Application and properties of siliceous mesostructured cellular foams as enzymes carriers to obtain efficient biocatalysts. *Micropor. Mesopor. Mat.* 99, 167-175. DOI: 10.1016/j.micromeso.2006.08.035
- [8] Amin, N., Gul, S., Sultana, S., Alam, S. (2021). Preparation and Characterization of Mesoporous Silica from Bagasse Bottom Ash from the Sugar Industry. *Crystals* 11, e11080938. DOI: 10.3390/cryst11080938
- [9] Naseem, T., Baig, M.M., Warsi, M.F., Hussain, R., Agboola, P.O., Waseem, M. (2021). Mesoporous silica prepared via a green route: a comparative study for the removal of crystal violet from wastewater. *Mat. Res. Exp.* 8, e015005. DOI: 10.1088/2053-1591/abd45d

- [10] Amin, N., Faisal, M., Saeedgul, K.M. (2016). Synthesis and characterization of geopolymer from bagasse bottom ash, waste of sugar industries and naturally available China clay. J. Clean. Prod. 129, 491-495. DOI: 10.1016/j.jclepro.2016.04.024
- [11] Affandi, S., Setyawan, H., Winardi, S., Purwanto, A., Balgis, R. (2009). A facile method for production of high-purity silica xerogels from bagasse ash. Adv. Powder Technol. 20, 468-472. DOI: 10.1016/j.apt.2009.03.008
- [12] Morales-Paredes, C.A., Rodríguez-Linzan, I., Saquete, M.D., Luque, L., Osman, S.M., Boluda-Botella, N., Manuel, R.D.J. (2023). Silica-derived materials from agro-industrial waste biomass: Characterization and comparative studies. *Environ. Res.* 231, 116002(1-8). DOI: 10.1016/j.envres.2023.116002
- [13] Pérez-Casas, J.A., Zaldívar-Cadena, A.A., Álvarez-Mendez, A., Ruiz-Valdés, J.J., Parra-Arciniega, S.M.D.L., López-Pérez, D.C., Sánchez-Vázquez, A.I. (2023). Sugarcane Bagasse Ash as an Alternative Source of Silicon Dioxide in Sodium Silicate Synthesis. *Materials* 16, 6327(1-9). DOI: 10.3390/ma16186327
- [14] September, L.A., Kheswa, N., Seroka, N.S., Khotseng, L. (2023). Green synthesis of silica and silicon from agricultural residue sugarcane bagasse ash – a mini review. RSC Adv. 13, 1370-1380. DOI: 10.1039/D2RA07490G
- [15] Hermanto, B.M., Noor, E., Arkemna, Y., Riani, E. (2017). Life Cycle Assessment of Silicon From Bagasse Ashes. *Brit. J. Env. Sci.* 5(3), 9-15. https://eajournals.org/bjes/vol-5-issue-3-june-2017/life-cycleassessment-silicon-bagasse-ashes/
- [16] Mamidi, V., Katakojwala, R., Mohan, S.V. (2025). Amorphous nano-silica from sugarcane bagasse ash – process optimization, characterization, and sustainability analysis. *Biomass Conv. Biorefin.* 15, 4059-4071. DOI: 10.1007/s13399-024-05548-8
- [17] Sukirna, I., Dhaneswara, D., Siregar, D.J., Fatriansyah, J.F., Sofyan, N., Yuwono, A.H., R. Muslih. (2024). Synthesis of Mesoporous Silica from Sugarcane Bagasse Ash Using Pluronic 123 as a Colorant Adsorbent for Brilliant Green. Evergreen, 11, 1366-1374. DOI: 10.5109/7183448
- [18] Dhaneswara, D., Tsania, A., Fatriansyah, J.F., Federico, A., Ulfiati, R., Muslih, R., Mastuli, M.S. (2024). Synthesis of Mesoporous Silica from Sugarcane Bagasse as Adsorbent for Colorants Using Cationic and Non-Ionic Surfactants. Int. J. Technol. 15 (2), 373-382. DOI: 10.14716/ijtech.v15i2.6721
- [19] Rahman, N.A., Widhiana, I., Juliastuti, S.R., Setyawan, H. (2015). Synthesis of mesoporous silica with controlled pore structure from bagasse ash as a silica source. *Colloids Surf. A: Physicochem. Eng. Asp.* 476, 1-7. DOI: 10.1016/j.colsurfa.2015.03.018

- [20] Hermida, L., Agustian, J. (2024). The application of conventional or magnetic materials to support immobilization of amylolytic enzymes for batch and continuous operation of starch hydrolysis processes. Rev. Chem. Eng. 40(1), 1-34. DOI: 10.1515/revce-2022-003
- [21] Grace, M. (2024). Enzyme Immobilization: Its Advantages, Applications and Challenges. *Enz. Eng.* 13 (2), 248-249.
- [22] Prabhakar, T., Giaretta, J. Zulli, R., Rath, R.J., Farajikhah, S., Talebian, S., Dehghani, F. (2025). Covalent immobilization: A review from an enzyme perspective. *Chem. Eng. J.* 503, 158054. DOI: 10.1016/j.cej.2024.158054
- [23]Robescu, M.S., Bavaro, (2025).Comprehensive Guide Enzyme to Immobilization: All You Need Know. to Molecules, 30, 939. DOI: 10.3390/molecules30040939
- [24] Zhao, D., Huo, Q., Feng, J., Chmelka, B.F., Stucky, G.D. (1998). Nonionic Triblock and Star Diblock Copolymer and Oligomeric Surfactant Syntheses of Highly Ordered, Hydrothermally Stable, Mesoporous Silica Structures. J. Am. Chem. Soc. 120, 6024-6036. DOI: 10.1021/ja974025i
- [25] Schmidt-Winkel, P., Glinka, C.J., Stucky, G.D. (2000). Microemulsion Templates for Mesoporous Silica. Langmuir 16, 356-361. DOI: 10.1021/la9906774
- [26] Choi, Y., Lee, J., Kim, J. (2015). Salt-assisted synthesis of mesostructured cellular foams consisting of small primary particles with enhanced hydrothermal stability. *Micropor. Mesopor. Mat.* 212, 66-72. DOI: 10.1016/j.micromeso.2015.03.029
- [27] Hermida, L., Abdullah, A.Z., Mohamed, A.R. Nickel functionalized mesostructured cellular foam (MCF) silica as a catalyst for solventless deoxygenation of palmitic acid to produce diesellike hydrocarbons, in Ed Méndez-Vilas A. (2013). andforMaterialsprocessesenergy: communicating currentresearchand technological developments. Spain. Formatex Research Centre. pp. 312-319.
- [28] Ma, J., Liu, Q., Chen, D., Wen, S., Wang, T. (2015). Synthesis and characterisation of poreexpanded mesoporous silica materials. *Micro Nano Lett.* 10, 140-144. DOI: 10.1049/mnl.2014.0413
- [29] Shi, Y., Li, B., Wang, P., Dua, R., Zhao, D. (2012). Micelle swelling agent derived cavities for increasing hydrophobic organic compound removal efficiency by mesoporous micelle@silica hybrid materials. *Micropor. Mesopor. Mat.* 155, 252-257. DOI: 10.1016/j.micromeso.2012.02.002
- [30] Hasanah, U., Wikarsa, S., Asyarie, S. (2021). Various Chloride Salt Addition in Mesoporous Material (SBA-15) Synthesis and Potential as Carrier for Dissolution Enhancer. Adv. Health Sci. Res. 40, 343-349. DOI: 10.2991/ahsr.k.211105.050

- [31] Sangteantong, P., Chainarong, K., Donphai, W., Chareonpanich, M. (2024). Green synthesis of surfactant-free mesoporous silica with strong hydrophilicity via metal salt modifications for moisture adsorption. *React. Chem. Eng.* 9, 816-824. DOI: 10.1039/D3RE00513E
- [32] Hermida, L., Abdullah, A.Z., Mohamed, A.R. (2013). Synthesis and Characterization of Mesostructured Cellular Foam (MCF) Silica Loaded with Nickel Nanoparticles as a Novel Catalyst. *Mater. Sci. Appl.* 4(1), 52-62. DOI: 10.4236/msa.2013.41007
- [33] Swar, S., Máková, V., Stibor, I. (2019). Effectiveness of Diverse Mesoporous Silica Nanoparticles as Potent Vehicles for the Drug L-DOPA. *Materials* e12193202. DOI: 10.3390/ma12193202
- [34] Coates, J. Interpretation of Infrared Spectra, A Practical Approach. in Meyers, R.A. (2000). Encyclopedia of Analytical Chemistry. Chichester. John Wiley & Sons Ltd. pp. 10815– 10837.
- [35] Stuart, B.H. (2004). Infrared Spectroscopy: Fundamentals and Applications, New York. John Wiley & Sons Inc. pp. 45-70.
- [36] Segneanu, A.E., Gozescu, I., Dabici, A.M., Sfirloaga, P., Szabadai, Z, Organic Compounds FT-IR Spectroscopy. in Uddin, J. Macro to Nano Spectroscopy. (2012). Rijeka. InTech Open. pp. 145-164.
- [37] Wehling, R.J. Chapter 23 Infrared spectroscopy Part IV. Spectroscopy. In Nielsen, S.S. Food analysis, Food Science Texts Series (2003). Boston. Springer. pp. 407-420.
- [38] Ali, S., Hossain, Z., Mahmood, S., Alam, R. (1990). Purification of glucoamylase from Aspergillus terreus. World J. Microbiol. Biotechnol. 6, 431-433. DOI: 10.1007/BF01202129
- [39] Svensson, B., Pederse, T.G., Svendsen, I.B., Sakai, T., Otiesen, M. (1982). Characterization of two forms of glucoamylase from Aspergillus niger. Carlsberg Res. Comm. 47:55-69. DOI: 10.1007/BF02907797
- [40] Slivinski, C.T., Vinicius, A., Machado, L., Iulek, J., Ayub, R.A., de Almeida, M.D. (2011).
   Biochemical Characterisation of a Glucoamylase from Aspergillus niger Produced by Solid-State Fermentation. Braz. Arch. Biol. Technol. 54(3), 559-568. DOI: 10.1590/S1516-89132011000300018
- [41] Li, D.C., Yang, Y.J., Peng, Y.L., Shen, C.Y. (1998). Purification and characterization of extracellular glucoamylase from the thermophilic *Thermomyces lanuginosus*. *Mycol. Res.* 102(5), 568-572. DOI: 10.1017/S0953756297005200
- [42] Rao, V.B., Sastri, N.V.B., Rao, P.V.S. (1981).
  Purification and characterization of a thermostable glucoamylase from the thermophilic fungus *Thermomyces lanuginosus*.

  Biochem. J. 193:379-387. DOI: 10.1042/bj1930379

- [43] Kanyalakrit, W., Koichi, N., Yuji, T. (1989). Raw-Starch-Digesting Glucoamylase from Amylomyces sp. 4-2 Isolated from Loogpang Kaomag in Thailand. J. Fac. Agricul. Kyushu Univ. 33, 177-187. DOI: 10.5109/23927
- [44] Palleros, D.R. (2000). Infrared Spectroscopy in Experimental Organic Chemistry. New York. Wiley.
- [45] Chen, G., Ma, Y., Su, P., Fang, B. (2012). Direct binding glucoamylase onto carboxyl-functioned magnetic nanoparticles. *Biochem. Eng. J.* 67, 120-125. DOI: 10.1016/j.bej.2012.06.002
- [46] Bayne, L., Ulijn, R.V., Halling, P.J. (2013). Effect of pore size on the performance of immobilised enzymes. *Chem. Soc. Rev.* 42, 9000-9010. DOI: 10.1039/C3CS60270B
- [47] Butterfield, A., Bhattacharyya, D., Daunert, S., Bachas, L. (2001). Catalytic biofunctional membranes containing site specifically immobilized enzyme arrays: a review. J. Membr. Sci. 181, 29-37. DOI: 10.1016/S0376-7388(00)00342-2
- [48] Dwevedi, A, Basics of Enzyme Immobilization. in Dwevedi, A. *Enzyme Immobilization*. (2016). Switzerland. Springer International Publishing. pp. 21-44.
- [49] Milosavić, N., Prodanović, R., Jovanović, S., Novakovic, I., Vujčić, Z. (2005). Preparation and characterization of two types of covalently immobilized amyloglucosidase. J. Serb. Chem. Soc. 70(5), 713-719. Website: https://doiserbia.nb.rs/img/doi/0352-5139/2005/0352-51390505713M.pdf
- [50] Milosavić, N.B., Prodanović, R.M., Jovanović, M.S., Vujčić, Z.M. (2004). Immobilization of Glucoamylase on Macroporous Sphesres. APTEFF 35, 207-214. Website: https://scindeks-clanci.ceon.rs/data/pdf/1450-7188/2004/1450-71880435207M.pdf
- [51] Milosavić, N.B., Prodanović, R.M., Jovanović, S.M., Vujčić, Z.M. (2007). Immobilization of glucoamylase via its carbohydrate moiety on macroporous poly(GMA-co-EGDMA). Enzyme Microb. Technol. 40, 1422-1426. DOI: 10.1016/j.enzmictec.2006.10.018

- [52] Panek, A., Pietrow, O., Synowiecki, J. (2012). Characterization of glucoamylase immobilized on magnetic nanoparticles. *Starch*, 64 (12), 1003-1008. DOI: 10.1002/star.201200084
- [53] Kovalenko, G.A., Perminova, L.V. (2008). Immobilization of glucoamylase by adsorption on carbon supports and its application for heterogeneous hydrolysis of dextrin. *Carbohyd. Res.* 343, 1202-1211. DOI: 10.1016/j.carres.2008.02.006
- [54] Kovalenko, G.A., Perminova, L.V., Terent'eva, T.G., Plaksin, G.V. (2007). Catalytic Properties of Glucoamylase Immobilized on Synthetic Carbon Material Sibunit. Appl. Biochem. Microbiol. 43 (4), 374-378. DOI: 10.1134/S0003683807040023
- [55] Zhao, G., Wang, J., Li, Y., Chen, X., Liu Y. (2011). Enzymes Immobilized on Superparamagnetic Fe<sub>3</sub>O<sub>4</sub>@Clays Nanocomposites: Preparation, Characterization, and a New Strategy for the Regeneration of Supports. J. Phys. Chem. C 115, 6350-6359. DOI: 10.1021/jp200156j
- [56] Zhao, G., Wang, J., Li. Y., Huang, H., Chen, X. (2012). Reversible immobilization of glucoamylase onto metal-ligand functionalized magnetic FeSBA-15. *Biochem. Eng. J.* 68, 159-166. DOI: 10.1016/j.bej.2012.04.009
- [57] Kalburcu, T., Tuzmen, M.N., Akgol, S., Denizli, A. (2014). Immobilized metal ion affinity nanospheres for α-amylase immobilization. *Turkish J. Chem.* 38, 28-40. DOI: 10.3906/kim-1301-87
- [58] Demirkan, E., Dincbas, S. Sevinc, N., Ertan, F. (2011). Immobilization of B. amyloliquefaciens α-amylase and comparison of some of its enzymatic properties with the free form. *Roman. Biotechnol. Lett.* 16, 6690. Website: https://rombio.unibuc.ro/wp-content/uploads/2022/05/16-6-3.pdf
- [59] Ashly, P.C., Joseph, M.J., Mohanan, P.V. (2011). Activity of diastase α-amylase immobilized on polyanilines (PANIs). Food Chem. 127, 1808-1813. DOI: 10.1016/j.foodchem.2011.02.068.